# Review of Power Electronics Components at Cryogenic Temperatures

Handong Gui, *Student Member, IEEE*, Ruirui Chen, *Student Member, IEEE*, Jiahao Niu, *Student Member, IEEE*, Zheyu Zhang, *Senior Member, IEEE*, Leon M. Tolbert, *Fellow, IEEE*, Fei (Fred) Wang, *Fellow, IEEE*, Benjamin J. Blalock, *Senior Member, IEEE*, Daniel Costinett, *Senior Member, IEEE*, and Benjamin B. Choi

***Abstract*—In order to apply power electronics systems to applications such as superconducting systems under cryogenic temperatures, it is necessary to investigate the characteristics of different parts in the power electronics system. This article reviews the influence of cryogenic temperature on power semiconductor devices including Si and wide bandgap switches, integrated circuits, passive components, interconnection and dielectric materials, and some typical cryogenic converter systems. Also, the basic theories and principles are given to explain the trends for different aspects of cryogenically cooled converters. Based on the review, Si active power devices, bulk Complementary metal-oxide-semiconductor (CMOS) based integrated circuits, nanocrystalline and amorphous magnetic cores, NP0 ceramic and film capacitors, thin/metal film and wirewound resistors are the components suitable for cryogenic operation. Pb-rich PbSn solder or In solder, classic printed circuit boards material, most insulation papers and epoxy encapsulant are good interconnection and dielectric parts for cryogenic temperatures.**

***Index Terms*—Cryogenic converter, integrated circuit, interconnection and dielectric material, power semiconductor device, passive components.**

## I. Introduction

IN GENERAL, there are two main motivations to use cryogenically-cooled power electronics systems [1], [2]. First, some special applications such as spacecraft based electronic systems or superconducting machines require cryogenic temperatures for their operation. In such applications, power electronics systems supply power to electric equipment or machines. Conventionally, the power electronics systems are placed inside some thermal insulation and the temperature is maintained at room temperature (∼300 K) [1]–[4]. However, the extra thermal insulation and temperature regulation increase the complexity, weight, volume and cost. Thus, it would be beneficial if the power electronics systems can also operate at cryogenic temperatures.

Second, research has already shown that some semiconductor devices have improved performance at low temperatures such as lower on-resistance and faster switching speed [1]–[3], [5]–[7], which means that making power electronics systems work at cryogenic temperatures can contribute to lower power dissipation and smaller volume and weight.

Generally speaking, the temperature can be called cryogenic when it is lower than 123 K. The low temperature environment can be created with the help of liquefied natural gas (111 K), liquid nitrogen (77 K) or liquid helium (4 K). Compared to power electronics systems at room temperature (∼300 K), the requirements at such cryogenic temperatures are similar, which mainly includes high efficiency, high reliability and high power density. However, due to the significant temperature change, both the static and dynamic characteristics of the parts in power electronics systems can change significantly.

A typical power converter mainly consists of the following:

1) power semiconductor devices, which include diodes and active switches such as power MOSFETs;
2) integrated circuits, which include analog parts and circuits in the control or gate drives;
3) passive components, which include transformers, inductors, capacitors and resistors in power or control circuits;
4) interconnection and dielectric materials, which include solder, printed circuit board (PCB) and insulation materials providing electrical or mechanical support for the converter.

It is essential to understand the properties of all the aspects mentioned above at cryogenic temperatures so that one can select proper parts for the design.

Some converters have been tested at cryogenic temperatures, and some of the characteristics of the aforementioned parts are reported [1]–[4], [8]–[16]. Performance of power semiconductor devices are shown in [1]–[4], [10], and [13], but they mainly focus on Si diodes and MOSFETs. Properties of integrated circuits

Manuscript received February 21, 2019; revised May 9, 2019, July 11, 2019, and September 6, 2019; accepted September 14, 2019. Date of publication October 1, 2019; date of current version February 11, 2020. This work was supported by the Boeing Company and NASA. This work made use of the Engineering Research Center Shared Facilities supported by the Engineering Research Center Program of the National Science Foundation (NSF) and U.S. Department of Energy under NSF Award Number EEC-1041877, and the CURENT Industry Partnership Program. Recommended for publication by Associate Editor K. Ngo. *(Corresponding author: Handong Gui.)*

H. Gui, R. Chen, J. Niu, L. M. Tolbert, F. Wang, B. J. Blalock, and D. Costinett are with the Department of Electrical Engineering and Computer Science, The University of Tennessee, Knoxville, TN 37996 USA (e-mail: hgui@vols.utk.edu; rchen14@vols.utk.edu; jniu3@vols.utk.edu; tolbert@utk.edu; fred.wang@utk.edu; bblalock@tennessee.edu; daniel.costinett@utk.edu).

Z. Zhang is with Zucker Family Graduate Education Center, Clemson University Restoration Institute, North Charleston, SC 29405 USA (e-mail: zheyu.zhang@ieee.org).

B. B. Choi is with NASA Glenn Research Center, Cleveland, OH 44135 USA (e-mail: benjamin.b.choi@nasa.gov).

Color versions of one or more of the figures in this article are available online at http://ieeexplore.ieee.org.

Digital Object Identifier 10.1109/TPEL.2019.2944781

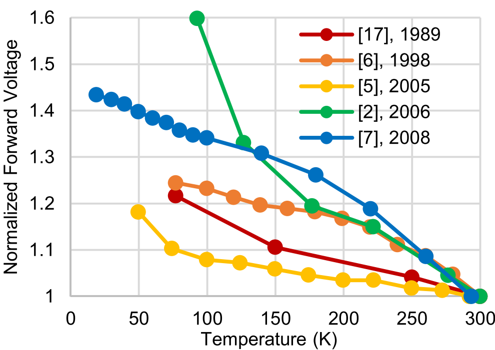


Fig. 1. Normalized forward voltage of Si *P–N* diodes.

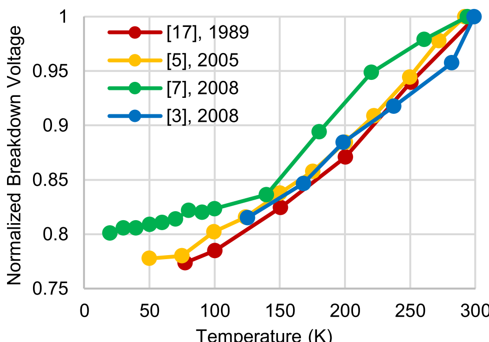


Fig. 2. Normalized breakdown voltage of Si *P–N* diodes.

are presented in [2]–[4], [8], and [9], while the characteristics of some passive components are analyzed in [1]–[4], [11]. However, most of these papers are more like testing reports without much theoretical analysis, and none of the existing literature covers all of the four different types of components mentioned earlier.

This article makes a comprehensive investigation of the existing literature on different parts in power electronics systems operating at cryogenic temperatures. Section II analyzes the characteristics of power semiconductor devices. Section III presents the behavior of integrated circuits. Section IV shows the features of passive components. Section V demonstrates the properties of interconnection and dielectric materials. Section VI provides a brief conclusion.

## II. Power Semiconductor Devices

Generally, the characterization of semiconductor devices at cryogenic temperature follows the rules and procedures at room temperature except that the device under test is located in a cryogenic chamber or vacuum station. The applied gate drives and conditioning circuits are identical to the testing at room temperature, so that the result can be fairly compared with the room temperature testing.

### A. Si P-N Diode

The Si P-N diode is one of the very first semiconductor devices developed for power circuits, and its performance at cryogenic temperatures has been investigated by several research groups [2], [3], [5]–[7], [17].

Fig. 1 plots the forward voltage of Si P-N diodes at different temperatures. The plotted value is normalized to that at room temperature. The forward voltage of a diode consists of the knee voltage and the voltage drop across the on-resistance. The knee voltage increases when the temperature decreases because of the drop in intrinsic carrier concentration at low temperature. Meanwhile, the on-resistance decreases when temperature drops from room temperature to around 100 K due to the increase of carrier mobility.

However, when temperature further decreases, the resistance increases because of the impact from carrier freeze-out [18]. Thus, the net effect can cause *P–N* diodes to exhibit different temperature coefficients depending on the current amplitude. Generally, within the current rating, the forward voltage shows negative temperature coefficient because the knee voltage is dominant as shown in Fig. 1. However, when the current is large enough, the on-resistance becomes dominant, and the forward voltage drop has positive temperature coefficient until the temperature is below 100 K.

Fig. 2 shows the normalized breakdown voltage of Si *P–N* diodes. The breakdown voltage declines because the mean free path of the carrier increases at low temperature, which contributes to higher impact ionization efficiency. So, more electron-hole pairs with high energy are created to launch impact ionization, and the avalanche is enhanced.

In terms of the switching performance of Si *P–N* diode at cryogenic temperatures, it is found that both the peak reverse current and the recovery time reduce due to the reduced carrier lifetime [6], [7].

### B. Si and SiC Schottky Diode

Unlike the *P–N* diode, Si and SiC Schottky diodes do not have a reverse recovery issue, which makes them more suitable for high switching frequency circuits. The temperature dependent forward voltage drop of Si and SiC Schottky diodes is similar to that of a Si *P–N* diode [2], [5], [6]. However, the on-resistance of SiC Schottky diodes increases more rapidly than Si Schottky diodes when the temperature is lower than 100 K due to larger influence by carrier freeze-out in SiC devices [2].

The breakdown voltage of Si and SiC Schottky diodes is stable or increases slightly at lower temperatures because of the reduced space charge generation caused by lower intrinsic carrier concentration [2], [6].

### C. Si MOSFET

Extensive testing and analysis have been conducted for Si power MOSFETs at cryogenic temperatures [6], [7], [19]–[27]. Fig. 3 demonstrates the normalized on-resistance of Si MOSFETs versus temperature. The on-resistance decreases significantly from room temperature to about 100 K due to the increased carrier mobility. However, the on-resistance increases as temperature drops below 100 K because of carrier freeze-out. For the same reason, the transconductance increases with decreasing temperature until around 100 K. The threshold voltage increases at low temperature because of the reduction of intrinsic carrier concentration. The body diode of the Si MOSFET is a Si *P–N* diode, so its behavior follows that of a Si *P–N* diode as analyzed earlier.

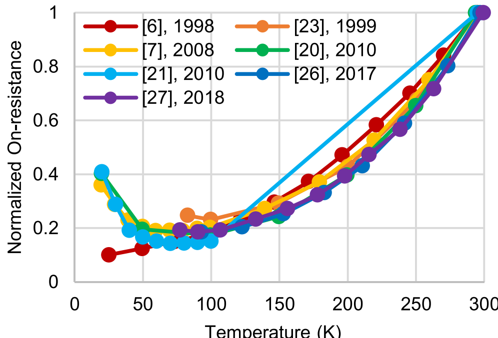


Fig. 3. Normalized on-resistance of Si MOSFETs.

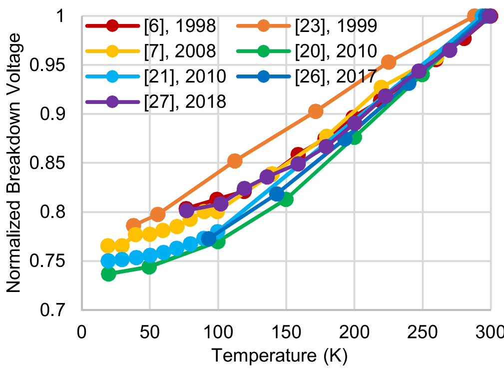


Fig. 4. Normalized breakdown voltage of Si MOSFETs.

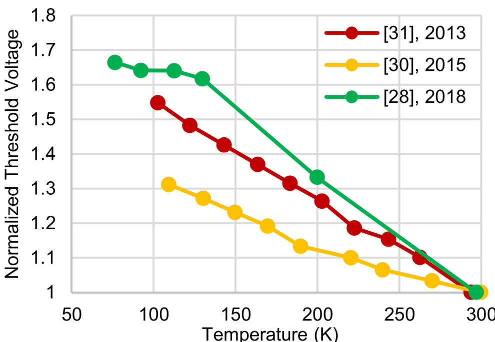


Fig. 5. Normalized threshold voltage of SiC MOSFETs.

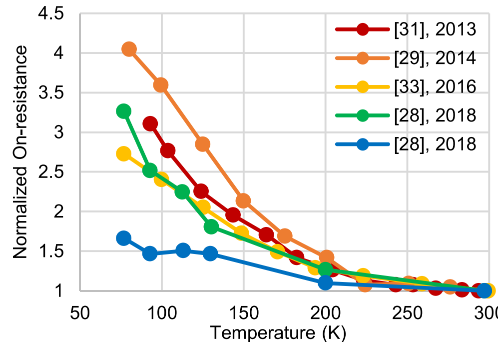


Fig. 6. Normalized on-resistance of SiC MOSFETs.

Fig. 4 gives the drain-source breakdown voltage of Si MOSFETs, and it reduces as the temperature drops. This is mainly due to the increase in the mean free path of carriers and higher impact ionization.

Due to the increased inversion layer mobility and its resultant higher transconductance, the switching speed can be faster and the switching loss can be reduced with lower temperature [26].

### *D. SiC MOSFET*

Wide bandgap devices are getting more and more popular because of their high thermal conductivity, high carrier mobility and saturated electron velocity compared to conventional Si devices. Among them, the silicon carbide (SiC) MOSFET is a strong competitor with the Si insulated gate bipolar transistor (IGBT) in similar voltage and power applications. At room temperature, SiC MOSFETs provide faster switching speed, lower switching loss and higher operating temperature. However, the existing research shows that SiC MOSFETs have relatively poor performance under cryogenic temperatures [28]–[35].

Fig. 5 illustrates the change of threshold voltage of SiC MOSFETs at different temperatures. Compared to the result by the conventional temperature dependent equation to calculate threshold voltage, the tested result appears to increase much more dramatically with the decrease of temperature. This phenomenon is related to the number of occupied interface traps. When the temperature decreases, the number of occupied interface traps increases rapidly, which results in the higher threshold voltage [31].

Fig. 6 shows the on-resistance of SiC MOSFETs at different temperatures. It is explained in [31] that the total on-resistance $R_{\text{total}}$ consists of two parts: the channel resistance $R_{\text{ch}}$ and the residual resistance $R_s$. $R_s$ includes the drift region, junction gate field-effect transistor (JFET), substrate and contact resistances, and is much larger than $R_{\text{ch}}$ at high temperature. $R_s$ drops with decreasing temperature due to higher carrier mobility similar to a Si MOSFET. However, $R_{\text{ch}}$ has a negative coefficient and becomes dominant at low temperature, which makes the total on-resistance increase rapidly. This is also caused by the increase of the interface state density since large amounts of electrons are trapped and few free electrons are available for conduction of the inversion layer. In addition, it is suggested by [32] that carrier freeze-out is also a contributor for the increase of on-resistance.

The drain-source breakdown voltage of a SiC MOSFET keeps relatively constant for a wide temperature range because the impact ionization efficiency does not increase [28]. It is reported that the switching speed of SiC MOSFETs does not improve or even gets worse at cryogenic temperatures [28], [30].

### *E. Gallium Nitride High Electron Mobility Transistor (GaN HEMT)*

In addition to SiC MOSFETs, GaN (HEMT) is another wide bandgap power device with appealing features at room temperature. Due to the different device structure compared to a MOSFET, GaN HEMT shows different characteristics under cryogenic temperatures [35]–[53].

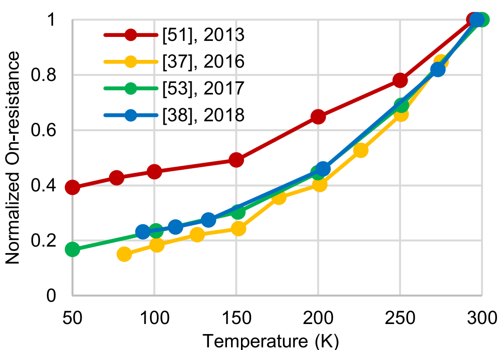


Fig. 7. Normalized on-resistance of GaN HEMTs.

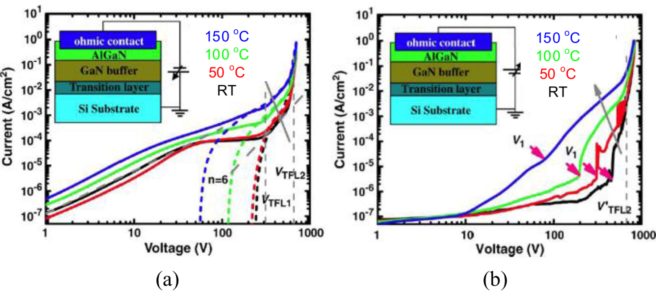


Fig. 8. Vertical breakdown behavior of GaN HEMT [48]. (a) Forward-biased. (b) Reverse-biased.

Fig. 7 shows the on-resistance of GaN HEMTs at different temperatures. It is observed that the on-resistance keeps decreasing with temperature. The on-resistance of the GaN HEMT $R_{\text{total}}$ mainly includes contact resistance of drain and source electrodes $R_c$, source to gate and gate to drain resistance $R_{\text{SG}}$ and $R_{\text{GD}}$ as well as the two-dimensional electron gas (2-DEG) channel resistance $R_{\text{ch}}$. Among them, $R_{\text{ch}}$ is the dominant part and is determined by the electron mobility in 2-DEG [41]. Due to the weak influence of Coulomb scattering, the electron mobility keeps increasing until the temperature reduces to around 40 K. Moreover, there is no sign of carrier freeze-out in GaN HEMTs due to the characteristics of 2-DEG at cryogenic temperatures. Therefore, the transconductance also increases with the decrease of temperature due to the increase of electron mobility.

The breakdown mechanism of GaN HEMTs is different from that of MOSFETs and is more complicated because of its lateral structure [45], [46], [52]. Several mechanisms can contribute to the breakdown of GaN HEMTs: source to drain punch-through, leakage through gate Schottky junction, vertical leakage of substrate, and impact ionization between source and drain [46].

Not much research has been conducted in analyzing the breakdown of GaN HEMTs at cryogenic temperatures. However, the temperature dependent trend shows that vertical leakage of the substrate is the dominant factor that impacts the breakdown behavior. Fig. 8 in [52] shows the forward and reverse biased breakdown behavior of a GaN HEMT. It can be seen that although the leakage current during the increase of voltage changes with temperature, the breakdown voltage keeps almost constant from 423 K to room temperature, which indicates that it is not caused by impact ionization. The potential reason for the vertical breakdown is that, electrons are injected from the substrate and trapped in the buffer. With the increase of voltage bias, the trapped carriers are ionized and more free electrons are generated. The relatively constant breakdown voltage of GaN HEMTs at cryogenic temperatures is verified in [38].

The threshold voltage of normally off p-GaN HEMTs should have positive temperature coefficient at low temperatures because the increase in intrinsic carrier concentration and ionization in the p-GaN layer and GaN buffer. This matches with the trend of devices from GaN Systems and Panasonic [38], [50]. However, $V_{th}$ of GaN field-effect transistor (FET) from Efficient Power Conversion Corp. (EPC) shows negative coefficient as reported in [37], whose reason is not reported.

The current collapse phenomenon (kink effect) due to the trapped electrons in the surface states is a potential issue for GaN HEMTs. Several papers have analyzed the kink effect at cryogenic temperatures [39], [42], [44], [47], [49]. It is found that the kink effect is more severe when the temperature decreases since lower temperature enhances the surface traps. However, it should be noted that the existing literature focuses on depletion mode GaN HEMTs with relatively small voltage and current rating instead of enhancement mode power GaN HEMTs. So, it is still not clear what the current collapse issue of power GaN HEMTs is at low temperature.

### *F. Si Insulated Gate Bipolar transistor (IGBT)*

Though SiC MOSFETs are attracting more and more attention, Si IGBT is still widely used in medium to high power applications due to its low cost and high reliability and availability. IGBTs combine the advantages of MOSFETs and bipolar junction transistor (BJTs) so they have lower voltage drop compared to MOSFETs and lower power for the gate drive compared to BJTs. Since the aforementioned review has shown that SiC MOSFETs are not good candidates for cryogenic application, it is of great importance if Si IGBTs can show superior performance at low temperature.

The main drawback of IGBTs at room temperature is the current tailing caused by the removal of excess carriers stored in the *N*- drift region. Consequently, the turn-OFF time of IGBTs is significantly increased, and the switching frequency of the converter is limited. The switching performance of IGBTs at cryogenic temperatures has been analyzed [5]–[7], [34], [54], [55]. As shown in Fig. 9, the normalized turn-OFF time of IGBTs is plotted for different temperatures. The turn-off time can reduce by 80% as temperature drops from 287 to 50 K, which means that the switching speed and loss of an IGBT at cryogenic temperatures are much improved compared to room temperature. The decrease of the tailing time with lower temperature is due to the reduction of an IGBT's inherent PNP transistor gain. Because the lifetime of minority carriers in IGBTs decreases at low temperature, the gain of inherent PNP transistor $\beta$ reduces and leads to faster decay of collector current.

The trend of static characteristics of IGBTs is similar to that of a Si MOSFET. When the temperature drops, the forward breakdown voltage decreases due to higher impact ionization

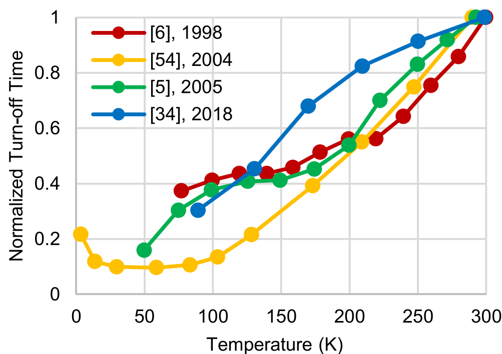


Fig. 9. Normalized turn-OFF time of Si IGBTs.

efficiency; the threshold voltage increases due to the reduction of intrinsic carrier concentration; the transconductance increases and the forward voltage drop decreases due to the increase of carrier mobility.

### *G. SiGe Diode and HBT*

The use of germanium (Ge) has been considered since the freeze-out temperature of dopants in Ge is much lower than in Si, and also the carrier mobility in Ge is higher than that in Si at low temperature [7].

Power semiconductor devices based on SiGe have been developed by GPD Optoelectronics Corp in cooperation with Auburn University, motivated by the NASA deep space exploration program [56], [57]. A 50 V/5 A SiGe heterojunction bipolar transistor was designed and fabricated, which was examined along with a SiGe diode in a 100 W, 24 V/48 V, 100 kHz boost power converter at low temperature. The dc current gain does not drop and the switching performance improves at cryogenic temperatures, which makes the SiGe heterojunction bipolar transistor (HBT) a promising candidate for cryogenic power converters.

However, some contradictory results are reported by the University of Akron and NASA with the same SiGe HBT in [58]. The testing shows that the dc current gain drops significantly when the temperature is lower than 200 K. Because there is no detailed description of the testing setup, applied device structure, and measurement methods, it is not clear why this result occurs. Before SiGe power devices can be utilized in real converters, much more device development and testing are needed.

### *H. Summary*

Figs. 10 and 11 compare the performance of diodes and active switches at cryogenic temperatures with their individual performance at room temperature. The specific performance at room temperature of each device is normalized to 1. A higher value at cryogenic temperatures means higher voltage, higher resistance, or longer switching time. Note that the value of the point indicates the relative increase or decrease in the characteristic of one device at cryogenic temperatures compared to its own characteristic at room temperature. For instance, the Si IGBT has larger switching time improvement at cryogenic temperatures than the Si MOSFET, so the IGBT has a lower point.

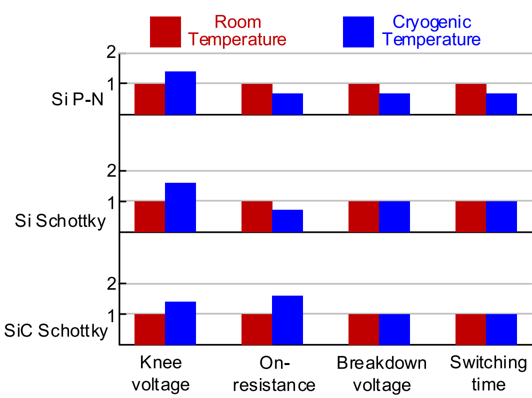


Fig. 10. Comparison of diodes' performance at cryogenic temperatures with their individual performance at room temperature.

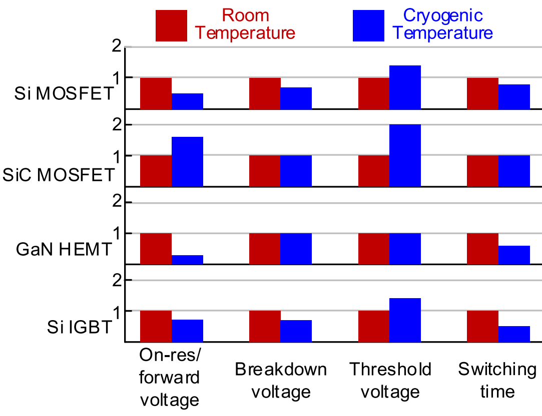


Fig. 11. Comparison of switches' performance at cryogenic temperatures with their individual performance at room temperature.

But it does not mean that at cryogenic temperatures, a Si IGBT can switch faster than a Si MOSFET. With the plotted comparison, it can be concluded that Si diodes, Si MOSFETs, GaN HEMTs and Si IGBTs can be adopted in cryogenic applications requiring lower loss, while SiC diodes and MOSFETs have poor conduction performance, but are more suitable for the cases requiring stable drain-source breakdown voltage.

## III. Integrated Circuits

### *A. Si BJT-Based*

Several papers have shown that Si BJTs perform poorly under low temperature [59]–[63], which means that integrated circuits based on BJTs are not suitable for cryogenic temperature operation.

Fig. 12 in [60] illustrates the dc current gain $\beta$ of a typical NPN BJT. It is clear that $\beta$ drops significantly with the decrease of temperature. This is mainly because the bandgap in emitter region drops at low temperature, which results in severe decrease of emitter injection efficiency. Another contributor is the reduction of base transport factor caused by the reduction of carrier lifetime.

As for other characteristics, the base-collector breakdown voltage decreases with decreasing temperature due to the typical

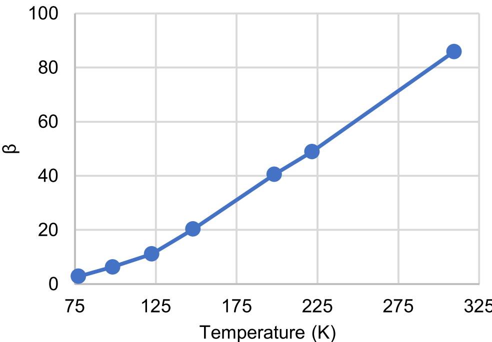


Fig. 12. DC current gain of BJT [60].

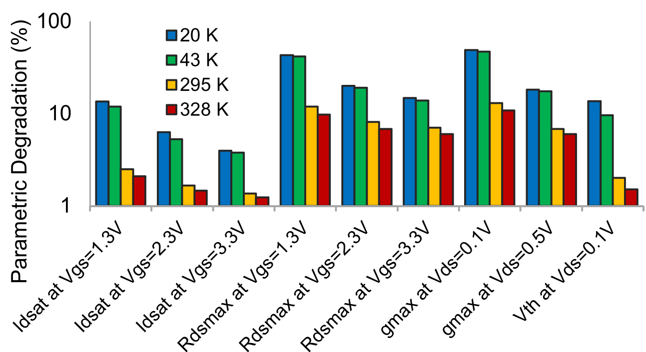


Fig. 13. Transconductance degradation of CMOS analog circuit [69].

*P–N* diode behavior. The collector-emitter breakdown voltage increases due to the reduced current gain. The switching speed increases because of the increase of diffusion coefficient and decrease of carrier lifetime. However, the advantage is not enough to compensate the decreased current gain.

### B. Bulk CMOS Based

Previous discussion indicates that power MOSFETs have improved performance at low temperature. For bulk Complementary metal-oxide-semiconductor (CMOS)-based integrated circuit, the main improvement is the switching speed [64]–[67]. Due to the increase of carrier mobility and saturation velocity at low temperature, the transconductance of both *n*-channel and *p*-channel MOSFETs increases. The unity gain frequency of bulk CMOS increases as temperature drops [68]. Therefore, bulk CMOS-based integrated circuits are more suitable for high frequency operation at cryogenic temperatures.

The absolute value of the threshold voltage of both *n*-channel and *p*-channel MOSFETs increase as temperature decreases because of the increased surface potential caused by decreased intrinsic carrier concentration.

Despite the benefit of faster switching speed brought by low temperature, reliability issues, such as gate degradation caused by hot carriers should be paid special attention to [66]–[70]. With increased carrier mobility and mean free path, the probability for carriers to gain enough energy to enter and get trapped in the gate oxide increases. Therefore, interface states are easier to be formed at low temperature, which is the source of transconductance degradation and threshold voltage shift. However, this phenomenon does not damage the device directly, but it limits the long-term reliability and lifetime. Fig. 13 from [69] shows the transconductance degradation of a CMOS analog circuit at different temperatures after the same operating time. The degradation increases when the temperature drops. The potential solution to mitigate the impact of hot carrier effect is to reduce the gate voltage at cryogenic temperatures so that the electric field is decreased, and the possibility for carriers to gain enough energy to flow into the gate oxide is reduced.

### C. SOI CMOS-Based

Silicon on insulator (SOI) technology can provide faster speed, lower power dissipation, and smaller package compared to conventional CMOS-based integrated circuits. Similar to bulk CMOS technology, the speed of the SOI device improves at low temperature. However, SOI devices suffer from kink effect at low temperature especially for partially depleted SOI [68], [71]–[73]. This phenomenon is one of the main floating body effects. Due to the higher impact ionization efficiency at low temperature, carriers are generated but they are not able to flow through the silicon substrate and part of them are trapped to form a forward bias of the body region, which reduces the threshold voltage and consequently increases the channel current. The kink effect decreases the voltage gain, increases loss, induces low frequency noise, and reduces lifetime of the device. This issue can be suppressed by using fully depleted SOI.

### D. SiGe HBT-Based

As mentioned above, SiGe HBT devices are expected to have better performance at cryogenic temperatures. Compared to power devices, there are more reports of SiGe technology in analog circuits [59], [74]–[78]. It has been shown that SiGe HBTs show significant increase in current gain with the decrease of temperature.

### E. Summary

It is concluded from the above review that bulk CMOS technology is promising for low temperature operation due to the higher switching speed capability, while the Si BJT is not suitable at cryogenic temperatures because of the significant degradation of current gain. Though SOI CMOS based and SiGe HBT-based technology also show some benefit at low temperature, they are not likely to be used in power converters due to the limited availability and cost issues since bulk CMOS operates acceptably.

## IV. Passive Components

### A. Inductors and Transformers

An inductor or transformer in a power converter mainly includes two parts: core and winding. Research has been conducted for different kinds of high frequency core material including powder, ferrite, nanocrystalline, and amorphous [79]–[91]. The comparison is given in Table I. Among them, ferrite core

TABLE I
COMPARISON OF DIFFERENT CORE MATERIALS AT CRYOGENIC TEMPERATURES WITH ROOM TEMPERATURE

| Material | Powder | | | Ferrite | Nano-crystalline | Amorphous |
|---|---|---|---|---|---|---|
| | MP | High Flux | Kool Mμ | | | |
| Permeability | -- | -- | ↓ | ↓↓ | ↑ | -- |
| Loss | ↑ | -- | -- | ↑↑ | ↑ | ↑ |
| Saturation flux density | N/A | N/A | N/A | Not clear | ↑ | ↑ |

↑↑: increase significantly ↑: increase slightly –: keep constant ↓: decrease slightly ↓↓: decrease significantly

shows the worst performance, which has significant decrease in permeability and increase in loss, making it not suitable for cryogenic applications. Different materials in powder cores show different characteristics. The permeability of molypermalloy (MP) and high flux core keeps constant while Kool M$\mu$ loses 40% of its permeability at 77 K. The loss of high flux and Kool M$\mu$ cores is relatively stable at low temperature while the loss of MP core increases by 40%. The amorphous and nanocrystalline cores have similar or even higher permeability and saturation flux density at cryogenic temperatures though the magnetic loss increases.

For the winding loss calculation, the anomalous skin effect is worth paying attention to [92]–[97]. According to the classical skin effect theory, the skin depth $\delta$ and the resistance at skin depth $R_s$ is expressed as

$$\delta = \sqrt{\frac{2}{\mu_0 \omega \sigma}} \qquad R_s = \sqrt{\frac{\mu_0 \omega}{2\sigma}} \tag{1}$$

where $\mu_0$ is the permeability of free space, $\omega$ is the angular frequency of current, and $\sigma$ is the dc conductivity.

It can be seen that the surface resistance is inversely proportional to the square root of the dc conductivity $\sigma$. Since $\sigma$ increases significantly at cryogenic temperatures, the resistance is expected to decrease. The classical theory is based on the current density equation

$$\vec{J} = \sigma \vec{E} \tag{2}$$

where $J$ is the current density and $E$ is the electric field. However, this equation is only valid when the skin depth is much longer than the mean free path of the electrons, which means that an electron does not experience electric field change before it collides. Meanwhile, at low temperature and high frequency applications, the mean free path of the electrons becomes even higher than the skin depth. In such case, the classical skin effect theory is not valid and the anomalous skin effect occurs.

With anomalous skin effect, the relationship between surface resistance and angular frequency of current is derived from [95]

$$R_s = \left(\frac{l}{\sigma}\right)^{\frac{2}{3}} \left(\frac{\sqrt{3\mu_0^2}}{16\pi}\right)^{\frac{1}{3}} \omega^{\frac{2}{3}} \tag{3}$$

where $l/\sigma$ is a constant depending on material. For copper, it equals to $6.8 \times 10^{-16}$ $\Omega\cdot$m$^2$. Thus, the surface resistance is independent of dc conductivity with the impact of anomalous skin effect. Fig. 14 shows the calculated surface resistance of the copper with residual resistivity ratio (RRR) equal to 2000

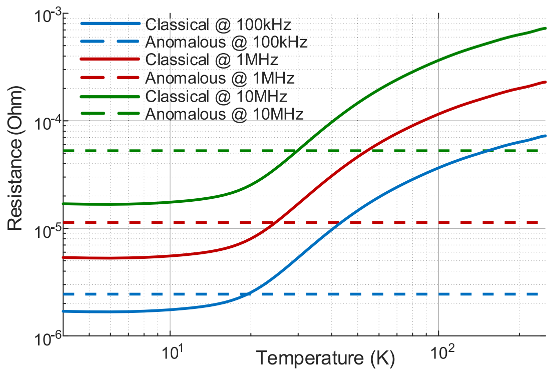


Fig. 14. Surface resistance with classical and anomalous skin effect of RRR = 2000 copper at different frequency.

based on classical and anomalous skin effect at 100 kHz, 1 MHz and 10 MHz, respectively. It is observed that at low temperature where the mean free path of the electron is larger than skin depth, the anomalous skin effect theory provides higher resistance than classical theory. With higher frequency, the distance between the result of anomalous theory and classical theory gets larger. Therefore, designers cannot depend only on classical skin effect theory to calculate winding loss since the anomalous skin effect can increase the ac winding resistance at low temperature and high frequency.

### B. Capacitors

Capacitors made from different materials operating at cryogenic temperatures have been investigated by several papers [2]–[4], [98]–[103]. Due to the difference in dielectric constant [98], capacitors can show different temperature dependent characteristics in capacitance and dissipation factor. Table II shows the change of capacitance and dissipation factors with temperature. It is concluded that NP0, polypropylene, polyphenylene sulfide (PPS), and mica perform well at cryogenic temperatures. For applications requiring high capacitance value, tantalum is preferred although its dissipation factor significantly increases while an electrolytic capacitor loses most of its capacitance at low temperature.

### C. Resistors

Resistors with different materials are compared at cryogenic temperatures in [2] and [3], and the results are shown in Table III. Thin film, metal film, and wirewound are good candidates for resistors while carbon and ceramic composition are poor at cryogenic temperatures.

TABLE II
COMPARISON OF DIFFERENT CAPACITORS AT CRYOGENIC TEMPERATURES WITH ROOM TEMPERATURE

| Material | Ceramic | | | | Film | | | | Mica | Electrolytic | Tantalum |
|---|---|---|---|---|---|---|---|---|---|---|---|
| | X7R | Y5V | Z5U | NP0 | Polypropylene | PPS | Polyester | Polycarbonate | | | |
| Capacitance | ↓↓ | ↓↓ | ↓↓ | -- | -- | -- | ↓ | ↓ | -- | ↓↓ | ↓ |
| Dissipation factor | ↑↑ | ↑↑ | ↑↑ | -- | ↓ | -- | ↓ | ↓ | -- | ↓↓ | ↑↑ |

↑↑: increase significantly ↑: increase slightly –: keep constant ↓: decrease slightly ↓↓: decrease significantly

TABLE III
COMPARISON OF DIFFERENT RESISTORS AT CRYOGENIC TEMPERATURES WITH ROOM TEMPERATURE

| Material | Thin film | Thick film | Metal film | Metal Oxide | Power film | Wirewound | Carbon Composition | Ceramic Composition |
|---|---|---|---|---|---|---|---|---|
| Resistance | -- | ↑ | -- | ↑ | ↑ | -- | ↑↑ | ↑↑ |

↑↑: increase significantly ↑: increase slightly –: keep constant

## V. INTERCONNECTION AND DIELECTRIC MATERIALS

### A. Solder

Solders provide both mechanical and electrical connection between dies, packages, and PCBs. Solder alloys are subject to cyclic stress resulting from mechanical or thermal cycling. The thermal expansion mismatch between the die or package and the substrate or PCB can cause the solder joints to deform and fatigue when cycled from room temperature to cryogenic temperatures.

Soft solder alloys are most widely used in power electronics applications since they have the advantage of lower melting temperature during assembly. However, they increase in strength and decrease in ductility with decreased temperature [104]–[107]. The most common soft solder is PbSn alloy, and it is able to operate at cryogenic temperatures and maintains its ductility if it has high Pb content. However, as Sn content increases up to more than 40%, the alloy becomes brittle at cryogenic temperatures. PbSn alloy containing Sb can mitigate this issue, but it is still not recommended to use Sn-rich solder for low temperature.

Compared to standard PbSn alloy, pure indium or indium alloys have shown to be much better at cryogenic temperatures due to the greater ductility and longer lifetime [105], [107]–[110]. So indium solder is the best candidate in soft solders if not considering the availability and cost.

In addition to soft solders, hard solders which are also called brazes, such as AuSn, AuGe, and AuSi alloys, have higher melting temperature and do not undergo stress but transmit more stress to die or package. Therefore, the device is more likely to crack during thermal cycling. However, it is found that AuSn can work well at cryogenic temperatures [111].

### B. Printed Circuit Boards

PCBs provide mechanical support, electrical connection as well as dielectric material in the circuit. They are usually made from glass fiber reinforced epoxy and can fatigue during thermal cycling due to thermal expansion mismatch. Based on the existing research [112]–[114], the fatigue occurs after more than 10 000 cycles at the pressure of 266 MPa, which is far beyond the normal operation environment. So the mechanical property of PCB material is strong enough to work for cryogenic applications.

The other concern is about the dielectric performance. Based on [115] and [116], the flashover breakdown voltage in liquid nitrogen is higher than that in transformer oil at room temperature. In conclusion, the mechanical and electrical performance of PCBs do not decline significantly at cryogenic temperatures.

TABLE IV
BREAKDOWN ELECTRIC FIELD OF DIELECTRIC MATERIALS AT CRYOGENIC TEMPERATURES

| Name | Material | $E_b$ (kV/mm) | Temp. (K) |
|---|---|---|---|
| Kapton | Polyimide | 230–360 | 12 |
| Teflon | Polytetrafluoroethylene | 230–310 | 12 |
| Mylar | Polyester | 190–300 | 12 |
| Nomex | Polyamide | 65–90 | 12 |
| Copaco rag | -- | 45–60 | 90 |
| Kraft paper | -- | 20–40 | 77 |

### C. Dielectric Paper

Table IV shows the breakdown electric field of some commonly used dielectric paper materials at cryogenic temperatures [116]–[121]. In general, most dielectric papers have improved dielectric performance at low temperatures, and they can be implemented in cryogenic applications.

### D. Encapsulants

Encapsulants are special dielectric materials that are widely used in power device packaging and busbar fabrication. The most common material for typical encapsulant is silicone gel-based and epoxy-based. However, silicone gel cannot survive at cryogenic temperatures [122]. It is found that partial discharge occurs when the temperature is lower than 215 K and can significantly reduce the breakdown voltage of the silicone gel. Moreover, the change of the breakdown voltage cannot be

TABLE V
CONVERTERS IN THE EXISTING LITERATURE

| Ref | Topology | Power (W) | Device | $f_s$ (kHz) |
|---|---|---|---|---|
| [2] | Full bridge | 20 | Si MOSFET | 20 |
| [3] | Full bridge | 24 | Si MOSFET | N/A |
| [11] | Switched capacitor | 1 k | GaN HEMT | 120 |
| [12] | Half bridge | 320 | Si MOSFET | 10 |
| [13] | Full bridge | 2.5k | Si MOSFET | 20 |
| [14] | Buck | 175 | Si MOSFET | 50 |
| [15] | Buck | 55 | Si MOSFET | 200 |
| [16] | Full bridge | 8 | Si MOSFET | 50 |

recovered even once the temperature returns to room temperature. Therefore, most commercially available power modules utilizing silicone gel-based encapsulants cannot be used for cryogenic applications. On the other hand, many epoxies can work at cryogenic temperatures [123]. The only issue is that epoxies tend to be more brittle as temperature drops. Thus, epoxies with lower moduli should be selected for operation at cryogenic temperatures.

## VI. CRYOGENIC CONVERTER SYSTEMS

Not many converters developed for cryogenic operation have been reported [2], [3], [11]–[16]. In general, the converters are tested inside a cryogenic chamber or box. The topologies, power rating, applied devices, and the switching frequencies are given in Table V.

The purpose of building these converters is mainly to verify the function and feasibility of the concept to run power converters at cryogenic temperatures, so the power ratings are normally low. Bridge type topologies are popular because most of them are for motor drives. Considering the device performance and availability, Si MOSFETs are mostly used, and the switching frequency is usually lower than 100 kHz. There is no reference about using Si IGBTs or SiC MOSFETs to build and run converters for high power applications at cryogenic temperatures.

It should be noted that, this article focuses on the properties of individual parts in power converter systems. However, interactions such as the coefficient of thermal expansion among the materials, components and systems are also essential and require special attention and calculation when developing cryogenic power converters.

## VII. CONCLUSION

This article reviewed the behavior of different parts in power electronics systems operating at cryogenic temperatures, which include power semiconductor devices, integrated circuits, passive components, interconnection, and dielectric materials. The characteristics, basic theory, and comparison are given for each part.

1) For power semiconductors, Si *P–N* diode shows improved on-resistance and switching performance at cryogenic temperatures, while the knee voltage and breakdown voltage decrease. Si Schottky diode has improved on-resistance but knee voltage increases, while a SiC Schottky diode has larger on-resistance at low temperature. Si MOSFET has smaller on-resistance and faster switching speed; however, the breakdown voltage decreases. SiC MOSFET shows poor performance at low temperature. GaN HEMT has improved on-resistance, switching speed and stable breakdown voltage. Si IGBT shows improved forward voltage drop and switching speed but lower breakdown voltage.
2) For integrated circuits, Si BJT has poor performance while bulk CMOS, SOI CMOS, and SiGe HBT work well at low temperatures. Considering the requirement of normal power electronics systems, bulk CMOS is the best candidate considering availability and cost.
3) In terms of passive components, ferrite core has poor performance at cryogenic temperatures while powder, amorphous and nanocrystalline cores can work at low temperature although the loss increases to some extent. Anomalous skin effect should be taken into consideration when calculating the winding loss. NP0 is the most suitable material for ceramic capacitors, while most film capacitors can work well at cryogenic temperatures. Both electrolytic and tantalum capacitors have worse performance. Metal film, thin film, and wirewound are candidates for resistors.
4) For interconnection and dielectric materials, Pb-rich PbSn or In alloys are preferred solders. Classical PCB is good enough for both mechanical and dielectric support. Most dielectric paper materials can work at cryogenic temperatures. Epoxy-based encapsulant is preferred. However, commercially available power modules with silicone gel encapsulant fail at cryogenic temperatures.
5) Existing cryogenic converter systems are mostly designed for low power and low voltage applications, and based on Si MOSFETs. The switching speed of the power devices is normally less than 100 kHz.

From the review, cryogenic temperature can cause significant change in properties of different materials, which results in the variation of the converter efficiency and reliability compared with room temperature case. Thus, designers need to carefully select materials for cryogenic applications, and this article can serve as initial guidance for designers to follow in building power electronics systems.

## REFERENCES

[1] K. Rajashekara and B. Akin, "A review of cryogenic power electronics-status and applications," in *Proc. IEEE Int. Elect. Mach. Drive*, 2013, pp. 899–904.
[2] J. Garrett, R. Schupbach, H. A. Mantooth, and A. B. Lostetter, "Development of an extreme environment DC motor drive full bridge power stage using commercial-off-the-shelf components," in *Proc. Int. Planetary Probe Workshop*, 2006.
[3] J. Bourne, R. Schupbach, B. Hollosi, J. Di, A. Lostetter, and H. A. Mantooth, "Ultra-wide temperature (-230°C to 130°C) DC-motor drive with SiGe asynchronous controller," in *Proc. IEEE Aerosp. Conf.*, 2008, pp. 1–15.
[4] M. Elbuluk and A. Hammoud, "Power electronics in harsh environments," in *Proc. Ind. Appl. Conf.*, 2005, vol. 2, pp. 1442–1448.
[5] S. Yang, "Cryogenic characteristics of IGBTs," Ph.D. Dissertation, Univ. of Birmingham, Birmingham, U.K., 2005.
[6] R. Singh and B. J. Baliga, *Cryogenic Operation of Silicon Power Devices*. New York NY, USA: Springer, 2012.

[7] C. Jia, "Experimental investigation of semiconductor losses in cryogenic DC-DC converters," Ph.D. Dissertation, Univ. of Birmingham, Birmingham, U.K 2008.
[8] M. Elbuluk, S. Gerber, A. Harnmoud, R. Patterson, and M. Newell, "Low temperature evaluation of bipolar-and CMOS-based current-mode PWM controllers," in *Proc. IEEE Conf. Ind. Electron. Soc.*, 2002, vol. 1, pp. 456–461.
[9] M. E. Elbuluk, A. Hammoud, S. Gerber, R. Patterson, and E. Overton, "Performance of high-speed PWM control chips at cryogenic temperatures," *IEEE Trans. Ind. Appl.*, vol. 39, no. 2, pp. 443–450, Mar./Apr. 2003.
[10] P. Haldar *et al.*, "Improving performance of cryogenic power electronics," *IEEE Trans. Appl. Supercond.*, vol. 15, no. 2, pp. 2370–2375, Jun. 2005.
[11] C. Barth *et al.*, "Experimental evaluation of a 1 kW, single-phase, 3-level gallium nitride inverter in extreme cold environment," in *Proc. IEEE Appl. Power Electron. Conf.*, 2017, pp. 717–723.
[12] C. Gold and C. J. Russo, "Cryogenic electronics power supply," U. S. Patent 5612615, Mar. 18. 1997.
[13] O. Mueller and K. Herd, "Ultra-high efficiency power conversion using cryogenic MOSFETs and HT-superconductors," in *Proc. IEEE Power Electron. Spec. Conf.*, 1993, pp. 772–778.
[14] B. Ray, S. S. Gerber, R. L. Patterson, and I. T. Myers, "Liquid nitrogen temperature operation of a switching power converter," NASA-TM-106867, 1995.
[15] B. Ray, S. S. Gerber, R. L. Patterson, and I. T. Myers, "77 K operation of a multi-resonant power converter," in *Proc. IEEE Power Electron. Spec. Conf.*, 1995, vol. 1, pp. 55–60.
[16] A. Forsyth, C. Jia, D. Wu, C. Tan, S. Dimler, Y. Yang, and W. Bailey, "Cryogenic converter for superconducting coil control," *IET Power Electron.*, vol. 5, no. 6, pp. 739–746, 2012.
[17] K. B. Hong and R. C. Jaeger, "Experimental survey of semiconductor power device operation at low temperature," in *Proc. Workshop Low Temp. Semicond. Electron.*, 1989, pp. 99–103.
[18] N. Ahmad, "Carrier freeze-out effects in semiconductor devices," *J. Appl. Phys.*, vol. 61, no. 5, pp. 1905–1909, 1987.
[19] M. Giesselmann, Z. Mahund, and S. Carson, "Investigation of power MOSFET switching at cryogenic temperatures," in *Proc. Int. Power Modulator Symp.*, 1996, pp. 47–50.
[20] K. Leong, A. T. Bryant, and P. A. Mawby, "Power MOSFET operation at cryogenic temperatures: Comparison between HEXFET, MDMesh TM, and CoolMOS TM," in *Proc. Int. Symp. Power Semicond. Devices, ICs*, 2010, pp. 209–212.
[21] K. Leong, B. Donnellan, A. Bryant, and P. Mawby, "An investigation into the utilisation of power MOSFETs at cryogenic temperatures to achieve ultra-low power losses," in *Proc. IEEE Energy Convers. Congr. Expo.*, 2010, pp. 2214–2221.
[22] O. Mueller, "Properties of high-power Cryo-MOSFETs," in *Proc. IEEE Ind. Appl. Conf.*, 1996, vol. 3, pp. 1443–1448.
[23] A. Schlogl, G. Deboy, H. Lorenzen, U. Linnert, H.-J. Schulze, and J. Stengl, "Properties of CoolMOS/sup TM/between 420 K and 80 K-the ideal device for cryogenic applications," in *Proc. Int. Symp. Power Semicond. Devices, ICs*, 1999, pp. 91–94.
[24] R. Singh and B. J. Baliga, "Power MOSFET analysis/optimization for cryogenic operation including the effect of degradation in breakdown voltage," in *Proc. Int. Symp. Power Semicond. Devices, ICs*, 1992, pp. 339–344.
[25] H. Ye, C. Lee, J. Raynolds, P. Haldar, M. J. Hennessy, and E. K. Mueller, "Silicon power MOSFET at low temperatures: A two-dimensional computer simulation study," *Cryogenics*, vol. 47, no. 4, pp. 243–251, 2007.
[26] Z. Zhang *et al.*, "Characterization of high-voltage high-speed switching power semiconductors for high frequency cryogenically-cooled application," in *Proc. IEEE Appl. Power Electron. Conf.*, 2017, pp. 1964–1969.
[27] Y. Chen *et al.*, "Experimental investigations of state-of-the-art 650-V class power MOSFETs for cryogenic power conversion at 77K," *IEEE J. Electron. Devices Soc.*, vol. 6, no. 1, pp. 8–18, Oct. 2018.
[28] H. Gui *et al.*, "Characterization of 1.2 kV SiC power MOSFETs at cryogenic temperatures," in *Proc. IEEE Energy Convers. Congr. Expo.*, 2018, pp. 7010–7015.
[29] T. Chailloux, C. Calvez, N. Thierry-Jebali, D. Planson, and D. Tournier, "SiC power devices operation from cryogenic to high temperature: Investigation of various 1.2 kV SiC power devices," *Mater. Sci. Forum*, vol. 778, pp. 1122–1125, 2014.
[30] H. Chen *et al.*, "Cryogenic characterization of commercial SiC Power MOSFETs," *Mater. Sci. Forum*, vol. 821, pp. 777–780, 2015.
[31] S. Chen, C. Cai, T. Wang, Q. Guo, and K. Sheng, "Cryogenic and high temperature performance of 4H-SiC power MOSFETs," in *Proc. IEEE Appl. Power Electron. Conf.*, 2013, pp. 207–210.
[32] H. Kim, J. Lim, and H. Cha, "DC characteristics of wide-bandgap semiconductor field-effect transistors at cryogenic temperatures," *J. Korean Phys. Soc.*, vol. 56, no. 5, pp. 1523–1526, 2010.
[33] S. Chowdhury, C. W. Hitchcock, and T. P. Chow, "Comparative evaluation of commercial 1200 V SiC power MOSFETs using diagnostic IV characterization at cryogenic temperatures," in *Proc. Eur. Conf. Silicon Carbide Related Mater.*, 2016, pp. 1–1.
[34] J. Qi *et al.*, "Dynamic performance of 4H-SiC power MOSFETs and Si IGBTs over wide temperature range," in *Proc. IEEE Appl. Power Electron. Conf.*, 2018, pp. 2712–2716.
[35] Z. Zhang *et al.*, "Characterization of wide bandgap device for cryogenically-cooled power electronics in aircraft applications," in *Proc. AIAA/IEEE Elect. Aircraft Technol. Symp.*, 2018, p. 5006.
[36] S.-J. Chang *et al.*, "Investigation of channel mobility in AlGaN/GaN high-electron-mobility transistors," *Jpn. J. Appl. Phys.*, vol. 55, no. 4, 2016, Art. no. 044104.
[37] J. Colmenares, T. Foulkes, C. Barth, T. Modeert, and R. C. Pilawa-Podgurski, "Experimental characterization of enhancement mode gallium-nitride power field-effect transistors at cryogenic temperatures," in *Proc. IEEE Workshop Wide Bandgap Power Devices Appl.*, 2016, pp. 129–134.
[38] R. Ren *et al.*, "Characterization of 650 V enhancement GaN HEMT at cryogenic temperatures," in *Proc. IEEE Energy Convers. Congr. Expo.*, 2018, pp. 891–897.
[39] R. Cuerdo *et al.*, "The kink effect at cryogenic temperatures in deep submicron AlGaN/GaN HEMTs," *IEEE Electron Device Lett.*, vol. 30, no. 3, pp. 209–212, Mar. 2009.
[40] M. Huque, S. Eliza, T. Rahman, H. Huq, and S. Islam, "Temperature dependent analytical model for current–voltage characteristics of AlGaN/GaN power HEMT," *Solid State Electron.*, vol. 53, no. 3, pp. 341–348, 2009.
[41] O. Katz, A. Horn, G. Bahir, and J. Salzman, "Electron mobility in an AlGaN/GaN two-dimensional electron gas. I. Carrier concentration dependent mobility," *IEEE Trans. Electron. Devices*, vol. 50, no. 10, pp. 2002–2008, Oct. 2003.
[42] J. K. Kaushik, V. R. Balakrishnan, B. S. Panwar, and R. Muralidharan, "On the origin of kink effect in current–voltage characteristics of AlGaN/GaN high electron mobility transistors," *IEEE Trans. Electron. Devices*, vol. 60, no. 10, pp. 3351–3357, Oct. 2013.
[43] M. Levinshtein *et al.*, "Mobility enhancement in AlGaN/GaN metal-oxide-semiconductor heterostructure field effect transistors," *Semicond. Sci. Technol.*, vol. 18, no. 7, p. 666, 2003.
[44] C.-H. Lin, W.-K. Wang, P.-C. Lin, C.-K. Lin, Y.-J. Chang, and Y.-J. Chan, "Transient pulsed analysis on GaN HEMTs at cryogenic temperatures," *IEEE Electron Device Lett.*, vol. 26, no. 10, pp. 710–712, Oct. 2005.
[45] B. Lu, E. L. Piner, and T. Palacios, "Breakdown mechanism in AlGaN/GaN HEMTs on Si substrate," in *Proc. Device Res. Conf.*, 2010, pp. 193–194.
[46] G. Meneghesso, M. Meneghini, and E. Zanoni, "Breakdown mechanisms in AlGaN/GaN HEMTs: An overview," *Jpn. J. Appl. Phys.*, vol. 53, no. 10, 2014, Art. no. 100211
[47] S. Nuttinck, S. Pinel, E. Gebara, J. Laskar, and M. Harris, "Cryogenic investigation of current collapse in AlGaN/GaN HFETS," in *Proc. Gallium Arsenide Appl. Symp.*, 2003, pp. 213–215.
[48] G. Parish *et al.*, "AlGaN/AlN/GaN high electron mobility transistors with improved carrier transport," in *Proc. Conf. Optoelectron. Microelectron. Mater. Devices*, 2004, pp. 29–32.
[49] H. Sun and C. Bolognesi, "Anomalous behavior of Al GaN/ GaN heterostructure field-effect transistors at cryogenic temperatures: From current collapse to current enhancement with cooling," *Appl. Phys.Lett.*, vol. 90, no. 12, 2007, Art. no. 123505.
[50] Y. Uemoto *et al.*, "Gate injection transistor (GIT)—A normally-off AlGaN/GaN power transistor using conductivity modulation," *IEEE Trans. Electron. Devices*, vol. 54, no. 12, pp. 3393–3399, Dec. 2007.
[51] X.-F. Zhang, L. Wang, J. Liu, L. Wei, and J. Xu, "Electrical characteristics of AlInN/GaN HEMTs under cryogenic operation," *Chin. Phys. B*, vol. 22, no. 1, 2013, Art. no. 017202.
[52] C. Zhou, Q. Jiang, S. Huang, and K. J. Chen, "Vertical leakage/breakdown mechanisms in AlGaN/GaN-on-Si devices," *IEEE Electron Device Lett.*, vol. 33, no. 8, pp. 1132–1134, Aug. 2012.

[53] R. E. Mayo, J. G. Bustamante, and T. L. Beechner, "Wide temperature range operation of GaN HEMTs for power dense energy conversion," in *Proc. IEEE Intersociety Conf. Thermal Thermomech. Phenomena Electron. Syst.*, 2017, pp. 530–536.

[54] A. Caiafa, A. Snezhko, J. Hudgins, E. Santi, and R. Prozorov, "IGBT operation at cryogenic temperatures: Non-punch-through and punch-through comparison," in *Proc. IEEE Power Electron. Spec. Conf.*, 2004, vol. 4, pp. 2960–2966.

[55] A. Caiafa, X. Wang, J. Hudgins, E. Santi, and P. Palmer, "Cryogenic study and modeling of IGBTs," in *Proc. IEEE Power Electron. Spec. Conf.*, 2003, vol. 4, pp. 1897–1903.

[56] R. Ward *et al.*, "Ge semiconductor devices for cryogenic power electronics: Part III," in *Proc. Int. Symp. Power Semicond. Devices, ICs*, 2003, pp. 321–324.

[57] R. Ward *et al.*, "SiGe semiconductor devices for cryogenic power electronics-IV," in *Proc. IEEE Appl. Power Electron. Conf.*, 2006, pp. 1673–1676.

[58] M. E. Elbuluk, A. Hammoud, and R. Patterson, "Performance of silicon germanium power devices at extreme temperatures," in *Proc. IEEE Power Electron. Spec. Conf.*, 2007, pp. 66–71.

[59] J. D. Cressler, "Silicon bipolar transistor: A viable candidate for high speed applications at liquid nitrogen temperature," *Cryogenics*, vol. 30, no. 12, pp. 1036–1047, 1990.

[60] W. P. Dumke, "The effect of base doping on the performance of Si bipolar transistors at low temperatures," *IEEE Trans. Electron. Devices*, vol. 28, no. 5, pp. 494–500, May. 1981.

[61] R. Singh and B. Baliga, "Cryogenic operation of power bipolar transistors," *Solid State Electron.*, vol. 39, no. 1, pp. 101–108, 1996.

[62] J. Stork, D. L. Harame, B. Mayerson, and T. N. Nguyen, "Base profile design for high-performance operation of bipolar transistors at liquid-nitrogen temperature," *IEEE Trans. Electron. Devices*, vol. 36, no. 8, pp. 1503–1509, Aug. 1989.

[63] J. Woo, J. D. Plummer, and J. Stork, "Non-ideal base current in bipolar transistors at low temperatures," *IEEE Trans. Electron. Devices*, vol. 34, no. 1, pp. 130–138, Jan. 1987.

[64] W. F. Clark, B. El-Kareh, R. Pires, S. Titcomb, and R. Anderson, "Low temperature CMOS-a brief review," *IEEE Trans. Compon. Packag. Manuf. Technol.*, vol. 15, no. 3, pp. 397–404, Jun. 1992.

[65] G. Ghibaudo and F. Balestra, "Low temperature characterization of silicon CMOS devices," in *Proc. Int. Conf. Microelectron.*, 1995, vol. 2, pp. 613–622.

[66] T. K. Makiniemi and P. Kosonen, "A low temperature pipelined analog-to-digital converter," in *Proc. IEEE Int. Conf. Electron. Circuits Syst.*, 2001, vol. 2, pp. 849–852.

[67] B. Okcan, P. Merken, G. Gielen, and C. Van Hoof, "A cryogenic analog to digital converter operating from 300 K down to 4.4 K," *Rev. Sci. Instrum.*, vol. 81, no. 2, p. 024702, 2010.

[68] F. Balestra and G. Ghibaudo, *Device and Circuit Cryogenic Operation for Low Temperature Electronics*. New York, NY, USA: Springer, 2013.

[69] Y. Chen *et al.*, "Design for ASIC reliability for low-temperature applications," *IEEE Trans. Device Mater. Rel.*, vol. 6, no. 2, pp. 146–153, 2006.

[70] A. Dejenfelt and O. Engström, "MOSFET mobility degradation due to interface-states, generatd by Fowler-Nordheim electron injection," *Microelectron. Eng.*, vol. 15, no. 1-4, pp. 461–464, 1991.

[71] C. Claeys and E. Simoen, "The perspectives of Silicon-on-Insulator technologies for cryogenic applications," *J. Electrochem. Soc.*, vol. 141, no. 9, pp. 2522–2532, 1994.

[72] C. Claeys and E. Simoen, "Perspectives of silicon-on-insulator technologies for cryogenic electronics," in *Perspectives, Science and Technologies for Novel Silicon on Insulator Devices*, New York, NY, USA: Springer, 2000, pp. 233–247.

[73] E. Simoen and C. Claeys, "The cryogenic operation of partially depleted silicon-on-insulator inverters," *IEEE Trans. Electron. Devices*, vol. 42, no. 6, pp. 1100–1105, Jun. 1995.

[74] B. Banerjee *et al.*, "Cryogenic operation of third-generation, 200-GHz peak-f/sub T/, silicon-germanium heterojunction bipolar transistors," *IEEE Trans. Electron. Devices*, vol. 52, no. 4, pp. 585–593, Apr. 2005.

[75] J. D. Cressler, "On the potential of SiGe HBTs for extreme environment electronics," *Proc. IEEE*, vol. 93, no. 9, pp. 1559–1582, Sep. 2005.

[76] Y. Lu and D. Heo, "Cryogenic performance of a 200 GHz SiGe HBT technology," in *Proc. Bipolar/BiCMOS Circuits Technol. Meeting*, 2003, pp. 171–173.

[77] S. Weinreb, J. C. Bardin, and H. Mani, "Design of cryogenic SiGe low-noise amplifiers," *IEEE Trans. Microw. Theory Techn.*, vol. 55, no. 11, pp. 2306–2312, Nov. 2007.

[78] Y. Yao, F. Dai, R. C. Jaeger, and J. D. Cressler, "A 12-bit cryogenic and radiation-tolerant digital-to-analog converter for aerospace extreme environment applications," *IEEE Trans. Ind. Electron.*, vol. 55, no. 7, pp. 2810–2819, Jul. 2008.

[79] M. Chen *et al.*, "The magnetic properties of the ferromagnetic materials used for HTS transformers at 77 K," *IEEE Trans. Appl. Supercond.*, vol. 13, no. 2, pp. 2313–2316, Jun. 2003.

[80] J. Claassen, "Inductor design for cryogenic power electronics," *IEEE Trans. Appl. Supercond.*, vol. 15, no. 2, pp. 2385–2388, Jun. 2005.

[81] M. Daniil, H. M. Fonda, and M. A. Willard, "Crystal structure and magnetic properties of (Fe, Si, Al)-based nanocomposite magnets designed for cryogenic applications," *Metall. Mater. Trans. E*, vol. 2, no. 2, pp. 139–145, 2015.

[82] M. Daniil, M. S. Osofsky, D. U. Gubser, and M. A. Willard, "(Fe, Si, Al)-based nanocrystalline soft magnetic alloys for cryogenic applications," *Appl. Phys.Lett.*, vol. 96, no. 16, 2010, Art. no. 162504.

[83] G. F. Dionne, "Properties of ferrites at low temperatures," *J. Appl. Phys.*, vol. 81, no. 8, pp. 5064–5069, 1997.

[84] S. S. Gerber, M. E. Elbuluk, A. Hammoud, and R. L. Patterson, "Performance of high-frequency high-flux magnetic cores at cryogenic temperatures," in *Proc. Intersociety Energy Convers. Eng. Conf.*, 2004, pp. 249–254.

[85] J. M. Niedra, "Comparative wide temperature core loss characteristics of two candidate ferrites for the NASA/TRW 1500 W PEBB converter," NASA/CR-1999-209302, 1999.

[86] J. M. Niedra and G. E. Schwarze, "Wide temperature magnetization characteristics of transverse magnetically annealed amorphous tapes for high frequency aerospace magnetics," NASA/TM-1999-209298, 1999.

[87] T. Pannaparayil, R. Marande, and S. Komarneni, "Magnetic properties of high-density Mn-Zn ferrites," *J. Appl. Phys.*, vol. 69, no. 8, pp. 5349–5351, 1991.

[88] J. Y. Park, L. K. Lagorce, and M. G. Allen, "Ferrite-based integrated planar inductors and transformers fabricated at low temperature," *IEEE Trans. Magn.*, vol. 33, no. 5, pp. 3322–3324, Sep. 1997.

[89] H. P. Quach and T. C. Chui, "Low temperature magnetic properties of Metglas 2714A and its potential use as core material for EMI filters," *Cryogenics*, vol. 44, no. 6, pp. 445–449, 2004.

[90] G. Rado, R. Wright, W. Emerson, and A. Terris, "Ferromagnetism at very high frequencies. IV. Temperature dependence of the magnetic spectrum of a ferrite," *Phys. Rev.*, vol. 88, no. 4, p. 909, 1952.

[91] M. Willard and T. Heil, "Cryogenic hysteretic loss analysis for (Fe, Co, Ni)–Zr–B–Cu nanocrystalline soft magnetic alloys," *J. Appl. Phys.*, vol. 101, no. 9, 2007, Art. no. 09N113.

[92] R. Chambers, "The anomalous skin effect," *Proc. Roy. Soc. London A, Math. Phys. Eng. Sci*., vol. 215, no. 1123, pp. 481–497, 1952.

[93] M. Kaganov, G. Y. Lyubarskiy, and A. Mitina, "The theory and history of the anomalous skin effect in normal metals," *Phys. Rep.*, vol. 288, no. 1, pp. 291–304, 1997.

[94] H. London, "Alternating current losses in superconductors of the second kind," *Phys. Lett.*, vol. 6, no. 2, pp. 162–165, 1963.

[95] E. Maxwell, "Superconducting resonant cavities," in *Advances in Cryogenic Engineering*, New York, NY, USA: Springer, 1961, pp. 154–165.

[96] A. Pippard, "The surface impedance of superconductors and normal metals at high frequencies. II. The anomalous skin effect in normal metals," *Proc. Roy. Soc. London A, Math. Phys. Eng. Sci.,* vol. 191, no. 1026, pp. 385–399, 1947

[97] G. Reuter and E. Sondheimer, "The theory of the anomalous skin effect in metals," *Proc. Roy, Soc. London A, Math. Phys. Eng. Sci.*, vol. 195, no. 1042, pp. 336–364, 1948.

[98] L. Faria, A. Passaro, L. Nohra, and R. d'Amore, "Influence of the cryogenic temperature and the BIAS voltage on the spontaneous polarization effect of X5R dielectric capacitors," *Proc. Int. Refereed J. Eng. Sci.*, vol. 1, no. 1, pp. 14–21, 2012.

[99] A. Hammoud, S. Gerber, R. L. Patterson, and T. L. MacDonald, "Performance of surface-mount ceramic and solid tantalum capacitors for cryogenic applications," in *Proc. IEEE Conf. Elect. Insul. Dielect. Phenom.*, 1998, vol. 2, pp. 572–576.

[100] A. Hammoud and E. Overton, "Low temperature characterization of ceramic and film power capacitors," in *Proc. IEEE Conf. Elect. Insul. Dielectr. Phenom.*, 1996, vol. 2, pp. 701–704.

[101] M.-J. Pan, "Performance of capacitors under DC bias at liquid nitrogen temperature," *Cryogenics*, vol. 45, no. 6, pp. 463–467, 2005.

[102] R. L. Patterson, A. Hammond, and S. S. Gerber, "Evaluation of capacitors at cryogenic temperatures for space applications," in *Proc. IEEE Int. Symp. Elect. Insul.*, 1998, vol. 2, pp. 468–471.

[103] F. Teyssandier and D. Prêle, “Commercially available capacitors at cryogenic temperatures,” in *Proc.Int. Workshop Low Temp. Electron.*, 2010.
[104] M. Abtew and G. Selvaduray, “Lead-free solders in microelectronics,” *Mater. Sci. Eng. R-Rep*, vol. 27, no. 5, pp. 95–141, 2000.
[105] R. W. Chang, *Influence of Cryogenic Temperature and Microstructure on Fatigue Failure of Indium Solder Joint*. College Park, MD, USA: Univ. Maryland, 2008.
[106] J. Ekin, *Experimental Techniques for low-Temperature Measurements: Cryostat Design, Material Properties and Superconductor Critical-Current Testing*. Oxford, U.K.: Oxford Univ. Press, 2006.
[107] R. K. Kirschman, W. M. Sokolowski, and E. A. Kolawa, “Die attachment for À120 C to 20 C thermal cycling of microelectronics for future Mars rovers—An overview,” *J. Electron. Packag.*, vol. 123, no. 2, pp. 105–111, 2001.
[108] R. W. Chang and F. P. McCluskey, “Reliability assessment of indium solder for low temperature electronic packaging,” *Cryogenics*, vol. 49, no. 11, pp. 630–634, 2009.
[109] M. Plötner, B. Donat, and A. Benke, “Deformation properties of indium-based solders at 294 and 77 K,” *Cryogenics*, vol. 31, no. 3, pp. 159–162, 1991.
[110] R. Reed, C. McCowan, R. Walsh, L. Delgado, and J. McColskey, “Tensile strength and ductility of indium,” *Mater. Sci. Eng. A*, vol. 102, no. 2, pp. 227–236, 1988.
[111] C. C. Lee and G. Matijasevic, “Highly reliable die attachment on polished GaAs surfaces using gold-tin eutectic alloy,” *IEEE Trans. Compon. Packag. Manuf. Technol.*, vol. 12, no. 3, pp. 406–409, Sep. 1989.
[112] W. Hwang and K. Han, “Statistical study of strength and fatigue life of composite materials,” *Composites*, vol. 18, no. 1, pp. 47–53, 1987.
[113] T. Takeda, S. Takano, Y. Shindo, and F. Narita, “Deformation and progressive failure behavior of woven-fabric-reinforced glass/epoxy composite laminates under tensile loading at cryogenic temperatures,” *Composites Sci. Technol.*, vol. 65, no. 11, pp. 1691–1702, 2005.
[114] C. Y. Yuan, H. C. Zhang, G. McKenna, C. Korzeniewski, and J. Li, “Experimental studies on cryogenic recycling of printed circuit board,” *Int. J. Adv. Manuf. Tech.*, vol. 34, no. 7, pp. 657–666, 2007.
[115] H. Rodrigo, D. Kwag, L. Graber, B. Trociewitz, and S. Pamidi, “AC flashover voltages along epoxy surfaces in gaseous helium compared to liquid nitrogen and transformer oil,” *IEEE Trans. Appl. Supercond.*, vol. 24, no. 3, pp. 1–6, Jun. 2014.
[116] E. Tuncer, G. Polizos, I. Sauers, and D. R. James, “Electrical insulation paper and its physical properties at cryogenic temperatures,” *IEEE Trans. Appl. Supercond.*, vol. 21, no. 3, pp. 1438–1440, Jun. 2011.
[117] F. Krahenbuhl *et al.*, “Properties of electrical insulating materials at cryogenic temperatures: A literature review,” *IEEE Elect. Insul. Mag.*, vol. 10, no. 4, pp. 10–22, Jul./Aug. 1994.
[118] J. Gerhold, “Properties of cryogenic insulants,” *Cryogenics*, vol. 38, no. 11, pp. 1063–1081, 1998.
[119] P. Chowdhuri, “Some characteristics of dielectric materials at cryogenic temperatures for HVDC systems,” *IEEE Trans. Elect. Insul.*, vol. EI-16, no. 1, pp. 40–51, Feb. 1981.
[120] I. Sauers, D. James, A. Ellis, and M. Pace, “High voltage studies of dielectric materials for HTS power equipment,” *IEEE Trans. Dielect. Elect. Insul.*, vol. 9, no. 6, pp. 922–931, Dec. 2002.
[121] J. Seong, I. Seo, J. Hwang, and B. Lee, “Comparative evaluation between DC and AC breakdown characteristic of dielectric insulating materials in liquid nitrogen,” *IEEE Trans. Appl. Supercond.*, vol. 22, no. 3, Jun. 2012, Art. no. 7701504.
[122] T. Vu, J.-L. Auge, and O. Lesaint, “Low temperature partial discharge properties of silicone gels used to encapsulate power semiconductors,” in *Proc. IEEE Conf. Elect. Insul. Dielect. Phenom.*, 2009, pp. 421–424.
[123] Epoxy Technology Inc. Cryogenic Temperature and Epoxies. 2015. [Online]. Available: http://www.epotek.com

**Handong Gui** (S’14) received the B.S. and M.S. degrees in electrical engineering from the Nanjing University of Aeronautics and Astronautics, Nanjing, China, in 2013 and 2016, respectively. He is currently working toward the Ph.D. degree with the University of Tennessee, Knoxville, TN, USA.

His research interests include wide band-gap devices and applications, multilevel converters, and electrified transportations.

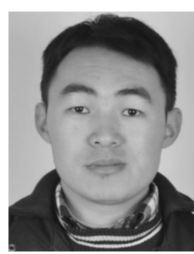

**Ruirui Chen** (S’15) received the B.S. degree from the Huazhong University of Science and Technology, Wuhan, China, and the M.S. degree from Zhejiang University, Hangzhou, China, in 2010 and 2013, respectively. He is currently working toward the Ph.D. degree with the University of Tennessee, Knoxville, TN, USA.

From 2013 to 2015, he was an Electrical Engineer with FSP-Powerland Technology Inc., Nanjing, China. His research interests include high power density converters for aircraft applications, multilevel converters, pulse width modulation techniques, converter paralleling control, and conducted EMI.

**Jiahao Niu** (S’16) received the B.S. degree in electrical engineering from Tsinghua University, Beijing, China in 2016. He is currently working toward the Ph.D. degree with the University of Tennessee, Knoxville, TN, USA.

His current research interests include design and control of high power ac drives, modular multilevel converters, wide bandgap semiconductors and their applications.

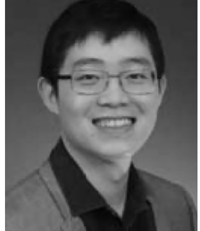

**Zheyu Zhang** (S’12–M’15–SM’19) received the B.S. and M.S. degrees from the Huazhong University of Science and Technology, Wuhan, China, and the Ph.D. degree from the University of Tennessee, Knoxville, TN, USA, in 2008, 2011, and 2015, respectively, all in electrical engineering.

He is the Warren H. Owen – Duke Energy Assistant Professor of engineering with Clemson University, Clemson, SC, USA. From 2015 to 2018, he was a Research Assistant Professor with the Department of Electrical Engineering and Computer Science with the University of Tennessee. From 2018 to 2019, he joined General Electric Research as the Lead Power Electronics Engineer at Niskayuna, NY, USA. He has authored or coauthored more than 80 papers in the most prestigious journals and conference proceedings, filed more than 10 patent applications with one licensed, authored one book and one book chapter, and presented four IEEE tutorial seminars. His research interests include wide band-gap based power electronics, modularity and scalability technology, medium voltage power electronics, advanced manufacturing and cooling technology (e.g., cryogenic cooling) applied in power electronics, and highly efficient, ultra-dense, cost-effective power conversion systems, for electric propulsion, electrified transportation, renewables, energy storage, and grid applications.

Dr. Zhang is currently an Associate Editor for the IEEE Transactions on Power Electronics and IEEE Transactions on Industry Applications. He was the recipient of two prize paper awards from the IEEE Industry Applications Society and IEEE Power Electronics Society.

**Leon M. Tolbert** (S'88–M'91–SM'98–F'13) received the bachelor's, M.S., and Ph.D. degrees in electrical engineering from the Georgia Institute of Technology, Atlanta, GA, USA, in 1989, 1991, and 1999, respectively.

From 1991 to 1999, he was with the Oak Ridge National Laboratory, Oak Ridge, TN, USA. He was an Assistant Professor with the Department of Electrical and Computer Engineering, University of Tennessee, Knoxville, TN, USA, in 1999. He is currently the Min H. Kao Professor in the Min H. Kao Department of Electrical Engineering and Computer Science, University of Tennessee. He is also a Founding Member of the NSF/DOE Engineering Research Center, Center for Ultra-Wide-Area Resilient Electric Energy Transmission Networks, UTK. He is also a part-time Senior Research Engineer with the Power Electronics and Electric Machinery Research Center, Oak Ridge National Laboratory.

Dr. Tolbert is a Registered Professional Engineer in the state of Tennessee. He was the recipient of the 2001 IEEE Industry Applications Society Outstanding Young Member Award, and six prize paper awards from the IEEE Industry Applications Society and IEEE Power Electronics Society. From 2007 to 2013, he was an Associate Editor for the IEEE TRANSACTIONS ON POWER ELECTRONICS. He was elected to serve as a Member-At-Large to the IEEE Power Electronics Society Advisory Committee for 2010–2012, the Chair of the PELS Membership Committee from 2011-2012, and a member of the PELS Nominations Committee from 2012-2014. He was the Paper Review Chair for the Industry Power Converter Committee of the IEEE Industry Applications Society from 2014 to 2017.

**Fei (Fred) Wang** (S'85–M'91–SM'99–F'10) received the B.S. degree from Xi'an Jiaotong University, Xi'an, China, and the M.S. and Ph.D. degrees from the University of Southern California, Los Angeles, in 1982, 1985, and 1990, respectively, all in electrical engineering.

From 1990 to 1992, he was a Research Scientist with the Electric Power Lab, University of Southern California. He joined the GE Power Systems Engineering Department, Schenectady, NY, USA, as an Application Engineer in 1992. From 1994 to 2000, he was a Senior Product Development Engineer with GE Industrial Systems, Salem, VA, USA. During 2000–2001, he was the Manager of Electronic and Photonic Systems Technology Lab, GE Global Research Center, Schenectady, NY ,USA, and Shanghai, China. In 2001, he joined the Center for Power Electronics Systems with Virginia Tech, Blacksburg, VA, USA, as a Research Associate Professor and became an Associate Professor in 2004. From 2003 to 2009, he was the CPES Technical Director. Since 2009, he has been with The University of Tennessee and Oak Ridge National Lab, Knoxville, TN, USA, as a Professor and the Condra Chair of Excellence in power electronics. He is a Founding Member and the Technical Director of the multiuniversity NSF/DOE Engineering Research Center for Ultra-wide-area Resilient Electric Energy Transmission Networks led by The University of Tennessee. His research interests include power electronics and power systems.

Dr. Wang is a fellow of the U.S. National Academy of Inventors.

**Benjamin J. Blalock** (S'86–M'97–SM'06) received the B.S. degree from the University of Tennessee, Knoxville, TN, USA, in 1991 and the M.S. and Ph.D. degrees from the Georgia Institute of Technology, Atlanta, GA, USA, in 1993 and 1996, respectively, all in electrical engineering.

He is the Blalock-Kennedy-Pierce Professor of analog electronics with the Department of Electrical Engineering and Computer Science, The University of Tennessee, where he directs the Integrated Circuits and Systems Laboratory. He has coauthored more than 200 refereed papers. His research focus at UT includes analog/mixed-signal integrated circuit design for extreme environments (both wide temperature and radiation) across multiple semiconductor technologies, ultra-low power analog signal processing, multichannel monolithic instrumentation systems, mixed-signal/mixed-voltage circuit design for systems-on-a-chip, and gate drive integrated circuits for wide bandgap (SiC and GaN) power electronics.

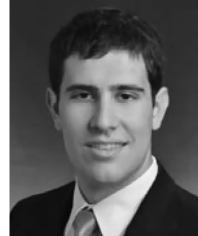

**Daniel Costinett** (S'10–M'13–SM'18) received the Ph.D. degree in electrical engineering from the University of Colorado, Boulder, CO, USA, in 2013.

He is currently an Associate Professor with the Department of Electrical Engineering and Computer Science, the University of Tennessee, Knoxville (UTK), Knoxville, TN, USA. Prior to joining UTK, he was an Instructor at Utah State University, in 2012. His research interests include resonant and soft switching power converter design, high efficiency wired and wireless power supplies, on-chip power conversion, medical devices, and electric vehicles.

Dr. Costinett is currently the Co-Director of education and diversity for the National Science Foundation/Department of Energy Research Center for Ultra-wide-area Resilient Electric Energy Transmission Networks. He is also a Joint Faculty with the Power Electronics and Electric Machinery Research Group, Oak Ridge National Laboratory. He was a recipient of the National Science Foundation CAREER Award in 2017. He is currently an Associate Editor for the IEEE JOURNAL OF EMERGING AND SELECTED TOPICS IN POWER ELECTRONICS, and IEEE TRANSACTIONS ON POWER ELECTRONICS.

**Benjamin B. Choi** received the B.S., M.S., and Ph.D. degrees from the University of Illinois, Champaign, IL, USA, in 1984, 1986, and 1990, respectively.

Since joining NASA GRC in 1990, he has been working on structural dynamics system modeling, analysis and control, especially in vibration control using magnetic bearing system and artificial intelligence technology for nearly 12 years. Since then, he started looking at the development of a bearingless motor technology for the electric propulsion system for future aircraft and NASA missions. He has also extended his research view into suppressing blade resonance using piezoelectric materials or shape memory alloy. During the last ten years, he has been involved in the propulsion electric grid simulator for future turboelectric distributed propulsion aircraft.